Efficacy of bortezomib in a direct xenograft model of primary effusion lymphoma

Kristopher A. Sarosiek[a,b], Lucas E. Cavallin[c], Shruti Bhatt[a,b], Ngoc L. Toomey[b], Yasodha Natkunam[d], Wilfredo Blasini[e], Andrew J. Gentles[f], Juan Carlos Ramos[b,c], Enrique A. Mesri[b,c], and Izidore S. Lossos[a,b,1]

Departments of [a]Molecular and Cellular Pharmacology and [b]Medicine, Division of Hematology-Oncology, Sylvester Comprehensive Cancer Center, [c]Microbiology and Immunology, and [e]Pathology, University of Miami Miller School of Medicine, Miami, FL 33136; and Departments of [d]Pathology and [f]Integrative Cancer Biology, School of Medicine, Stanford University, Stanford, CA 94305

Edited* by Ronald Levy, Stanford University, Stanford, CA, and approved June 14, 2010 (received for review March 8, 2010)

Primary effusion lymphoma (PEL) is an aggressive B-cell lymphoma most commonly diagnosed in HIV-positive patients and universally associated with Kaposi's sarcoma-associated herpesvirus (KSHV). Chemotherapy treatment of PEL yields only short-term remissions in the vast majority of patients, but efforts to develop superior therapeutic approaches have been impeded by lack of animal models that accurately mimic human disease. To address this issue, we developed a direct xenograft model, UM-PEL-1, by transferring freshly isolated human PEL cells into the peritoneal cavities of NOD/SCID mice without in vitro cell growth to avoid the changes in KSHV gene expression evident in cultured cells. We used this model to show that bortezomib induces PEL remission and extends overall survival of mice bearing lymphomatous effusions. The proapoptotic effects of bortezomib are not mediated by inhibition of the prosurvival NF-κB pathway or by induction of a terminal unfolded protein response. Transcriptome analysis by genomic arrays revealed that bortezomib down-regulated cell-cycle progression, DNA replication, and Myc-target genes. Furthermore, we demonstrate that in vivo treatment with either bortezomib or doxorubicin induces KSHV lytic reactivation. These reactivations were temporally distinct, and this difference may help elucidate the therapeutic window for use of antivirals concurrently with chemotherapy. Our findings show that this direct xenograft model can be used for testing novel PEL therapeutic strategies and also can provide a rational basis for evaluation of bortezomib in clinical trials.

Kaposi's sarcoma-associated herpesvirus | Herpesvirus 8

Primary effusion lymphoma (PEL) is a distinct and aggressive subtype of non-Hodgkin's lymphoma (NHL) universally associated with infection by Kaposi's sarcoma-associated herpesvirus (KSHV), also called "human herpesvirus-8" (HHV-8) (1, 2). PEL most commonly presents with pleural, peritoneal, or pericardial malignant effusions without a contiguous tumor mass (3). Rarely, PEL also may develop as an isolated solid tumor mass exhibiting a morphology, immunophenotype, and gene-expression profile similar to classical liquid-phase PEL (4). This lymphoma is diagnosed most commonly in HIV-positive patients, accounting for 4% of all NHLs in this population, but also may develop in immunosuppressed HIV-negative individuals (5, 6).

Although KSHV is directly implicated in the oncogenesis of this lymphoma, most PEL cases also are associated with EBV (7), and the combination of the two may facilitate transformation. The majority of tumor cells in PEL are latently infected with KSHV, but a small subset undergoes spontaneous lytic replication (8). Latent infection is characterized by expression of the major latent transcripts which include latency-associated nuclear antigen-1 (*LANA-1*), viral Fas-associated with death domain (FADD)–like interleukin-1β–converting enzyme (FLICE)/caspase 8–inhibitory protein (*vFLIP*), and viral cyclin (*v-CYC*). LANA-1 is necessary for maintenance of the viral episome (9). The lytic phase of KSHV infection, which results in viral replication and cell lysis (10), is associated with increased expression of early and late lytic genes such as *RTA*, *vIL-6*, and *K8.1* (11). Studies have shown that KSHV-encoded *vFLIP* is essential for PEL survival by activating the antiapoptotic genes downstream of NF-κB (12).

The optimal therapy for PEL is unknown because the disease is rare and data from large-scale clinical trials are lacking. The lack of optimized therapy combined with the aggressive nature of PEL results in a short median survival of only 6 mo (13), underscoring the urgent need for development of new therapeutics. Currently, cyclophosphamide, doxorubicin, vincristine, and prednisone (CHOP) chemotherapy is used frequently as a first-line therapy for PEL, leading to short-lived remissions in only 43% of patients (5). In HIV-positive patients, highly active antiretroviral therapy (HAART) can induce lymphoma remission and is associated with a better prognosis (13). Recently, several new therapeutic strategies based on in vitro and in vivo studies of PEL have been proposed. These strategies include activating TNF-related apoptosis-inducing ligand (TRAIL)–mediated apoptosis by IFN-α and azidothymidine (14, 15), inhibiting NF-κB (16, 17), or administering antiviral therapy concomitantly with activation of lytic viral replication (18).

Several factors have limited progress in understanding and effectively treating PEL. Because the disease is rare, many studies have been performed only on PEL cell-line models that may deviate from the original tumor behavior in patients. Indeed, it has been shown that PEL depends on the tumor microenvironment for canonical growth, because in vitro cell-culture conditions can lead to KSHV and host gene-expression signatures that differ from patterns observed in vivo (19). These culture-induced changes in expression of KSHV-associated genes also have been documented at the protein level (20). Therefore improved models are needed that may reflect primary tumors more accurately. In an attempt to create an improved in vivo model system for elucidation of PEL pathogenesis and evaluation of novel therapeutic strategies, our laboratory recently developed a PEL mouse model (UM-PEL-1) that was established without ex vivo propagation of the human PEL cells to avoid culture-induced changes in KSHV gene expression. This model mimics human disease more accurately and may serve as a valuable tool for the study of this malignancy. Additionally, we showed that bortezomib treatment induces KSHV lytic reactivation and is a potent anti-PEL tumor agent. These findings warrant initiation of clinical studies of bortezomib alone or in combination with antivirals in patients with PEL.

Author contributions: K.A.S., L.E.C., E.A.M., and I.S.L. designed research; K.A.S., L.E.C., S.B., N.L.T., Y.N., and W.B. performed research; K.A.S., L.E.C., S.B., N.L.T., Y.N., W.B., A.J.G., J.C.R., E.A.M., and I.S.L. analyzed data; and K.A.S., A.J.G., and I.S.L. wrote the paper.

The authors declare no conflict of interest.

*This Direct Submission article had a prearranged editor.

Data deposition: The data reported in this paper have been deposited in the Gene Expression Omnibus (GEO) database, www.ncbi.nlm.nih.gov/geo (accession no. GSE22594).

[1]To whom correspondence should be addressed. E-mail: ilossos@med.miami.edu.

This article contains supporting information online at www.pnas.org/lookup/suppl/doi:10.1073/pnas.1002985107/-/DCSupplemental.

Results

Case Report. An 86-y-old HIV-negative white male with extensive cardiovascular disease and renal failure presented with weight loss, shortness of breath, and a right pleural effusion. A pleural tap led to a diagnosis of B-cell PEL based on the presence of atypical lymphoid cells that stained positive for CD45, CD30, CD38, CD138, HLA-DR, HHV-8 (LANA1), and Epstein–Barr encoded RNA (EBER) (Figs. S1 and S2 and Table S1). CD3, CD19, CD20, and CD79a staining was negative. A monoclonal rearrangement of the B-cell receptor and a complex karyotype (Fig. S1*B*) confirmed the diagnosis. The patient received doxorubicin (Adriamycin) and bortezomib therapy and demonstrated a marked decrease in pleural effusion. However, the patient developed neutropenic sepsis and died within 30 d of diagnosis.

Development of the UM-PEL-1 in Vivo Model. PEL cells (2×10^7) obtained from the diagnostic tap of the aforementioned patient were injected into the peritoneal cavities of immunodeficient NOD/SCID mice immediately after retrieval. Injected mice developed peritoneal swelling within 5–7 d, whereas mock-injected mice did not (Fig. 1*A*). Mice injected with PEL cells and then untreated became moribund because of disease within 2–3 wk. The in vivo PEL model could be propagated via collection of PEL cells from ascites (referred to as "UM-PEL-1 cells") and injection into peritoneal cavities of naïve mice with a 100% engraftment rate (72 of 72 injected mice). Cell-surface antigen expression was monitored in sequential xenografts to ensure maintenance of PEL phenotype.

Histological Findings. Peritoneal effusions as well as solid lymphomas were evident in mice at postmortem analysis, and tumor nodules were found on peritoneal or serosal surfaces or in association with the omentum (Fig. 1*B*). Some tumors infiltrated the parenchyma of the pancreas or bowel wall smooth muscle (Fig. 1*C*). No involvement of the spleen, bone marrow, lymph node, lung, liver, or kidney was seen. Tumor cells were medium to large in size with pleomorphic nuclear outlines, prominent nucleoli, moderate to abundant cytoplasm, and an immunophenotype identical to the primary PEL cells (Fig. 1 *D*–*J*). PCR analysis showed a monoclonal V_H4–34 IgG heavy chain with 83% homology to the germ line and evidence of antigen selection. The UM-PEL-1 karyotype depicted in Fig. S1*B* was identical to the karyotype of the primary cells and demonstrated 51, XY, dup(1)(q22q31), +4, +5, +7, +19, add(21)(p13). UM-PEL-1 cells derived from mice ascites also could grow and be propagated in vitro; these cells were designated "UM-PEL-1c."

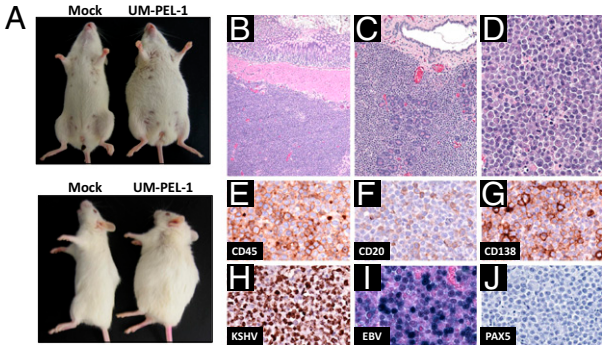

Fig. 1. Establishment and characterization of UM-PEL-1. (*A*) Mice 7 d after mock injection or injection with UM-PEL-1 cells. (*B* and *C*) H&E-stained sections of mouse tissue show a tumor nodule on the serosal surface of the bowel wall (*B*) and tumor cells infiltrating pancreatic parenchyma (*C*). (*D*) Tumor cells are medium to large with pleomorphic nuclear outlines, prominent nucleoli, and abundant cytoplasm and exhibit plasmacytoid differentiation. (*E*–*J*) Immunohistologic stains show that the tumor cells are positive for CD45 (*E*), weakly positive to absent CD20 (*F*), and strongly positive for CD138 (*G*). Tumor cells also harbor KSHV (*H*) and EBV RNA detected by an in situ EBER probe (*I*). Tumor cells lack the B-cell transcription factor PAX5 (*J*). (Original magnifications: *B* and *C*, 100×; *D*–*J*, 600×.)

UM-PEL-1 Cells Are Infected with KSHV. Immunofluorescence antibody analysis for KSHV LANA showed that UM-PEL-1 cells freshly isolated from mouse ascites or solid tumors exhibited the classic punctate pattern indicative of episomal KSHV (Figs. 2*A* and 3*A*). In addition, cells and tumors uniformly expressed the latent gene *Kaposin* (*ORF K12*). A fraction of UM-PEL-1 cells expressed the late lytic viral gene *K8.1*, which generally is the consequence of spontaneous lytic reactivation (Fig. 3*A*). Similar to other PEL cell lines, UM-PEL-1 can be induced lytically by the addition of the histone deacetylase inhibitor trichostatin A (TSA), causing a significant increase in the expression of the lytic transactivator gene *RTA* and *K8.1* (Fig. 2 *B* and *C*). Cell-free TSA-induced supernatants were able to transfer KSHV to Vero cells, indicating that UM-PEL-1 cells bear infectious KSHV virions (Fig. 2 *D* and *E*). Comparative analysis of UM-PEL-1c cultured cells and UM-PEL-1 ascites and solid tumors carried out by real-time quantitative PCR (qPCR) showed variations in KSHV latent and lytic gene expression. UM-PEL-1c cells express more latent and lytic genes in vitro, whereas ascites and tumors show intermediate levels of expression (Fig. 3*B*). Relative viral load measurements showed the same trend (Fig. 3*C*). Taken together, these data further suggest that different microenvironments (in vitro versus in vivo) affect KSHV copy number and expression patterns.

Bortezomib Induces Apoptosis of UM-PEL-1 Cells. We set out to use the UM-PEL-1 cells to compare the efficacies of established and proposed PEL therapies. We therefore evaluated the anti-PEL activity of bortezomib and doxorubicin. Direct comparisons of these therapies were conducted on UM-PEL-1c cells that were collected from mice and propagated in vitro in standard culture conditions. These cells were treated with the chemotherapies for up to 72 h, and cell viability was assessed by flow cytometric analysis. Although treatment with doxorubicin as well as bortezomib reduced UM-PEL-1c cell viability, the latter induced higher levels of apoptosis at earlier time points at clinically achievable concentrations (Fig. 4*A* and Fig. S3). Induction of apoptosis with either treatment was dose and time dependent, and a majority of UM-PEL-1c cells were sensitive to either treatment.

Bortezomib Enhances Survival of Mice Bearing PEL Xenografts. Although bortezomib induced apoptosis more potently than doxorubicin in UM-PEL-1c cells in vitro, in vivo studies were necessary to compare the efficacies of the two chemotherapies because of the substantial changes in the KSHV and host transcriptome during ex vivo culture. To this end, UM-PEL-1 cells were used to establish lymphomatous effusions in the peritoneal cavities of NOD/SCID mice. On the third day after injection of UM-PEL-1 cells, mice began receiving twice-weekly i.p. injections of PBS, bortezomib, or doxorubicin for 3 wk. Mice were monitored daily. In vivo treatment of the UM-PEL-1–bearing mice with bortezomib (0.3 mg/kg) was well tolerated and improved mouse overall survival compared with control animals treated with PBS ($P < 0.01$; median survival of bortezomib-treated mice was 32 d, compared with 15 d in controls) (Fig. 4*B*). I.p. doxorubicin injections (1.25 mg/kg) at the same treatment intervals resulted in a median survival of 24 d, significantly inferior to median survival with bortezomib ($P = 0.035$). Because viral biology is intricately linked to PEL survival, we interrogated the effects of the therapies on KSHV gene expression. We found that in vivo both bortezomib and doxorubicin led to an increase in the overall KSHV gene expression, including up-regulation of the lytic transactivator *RTA*, early lytic genes *ORF49*, *ORF57*, and *vGPCR* and late lytic genes *K8.1* and glycoprotein B (*gB*) (Fig. 4 *C*

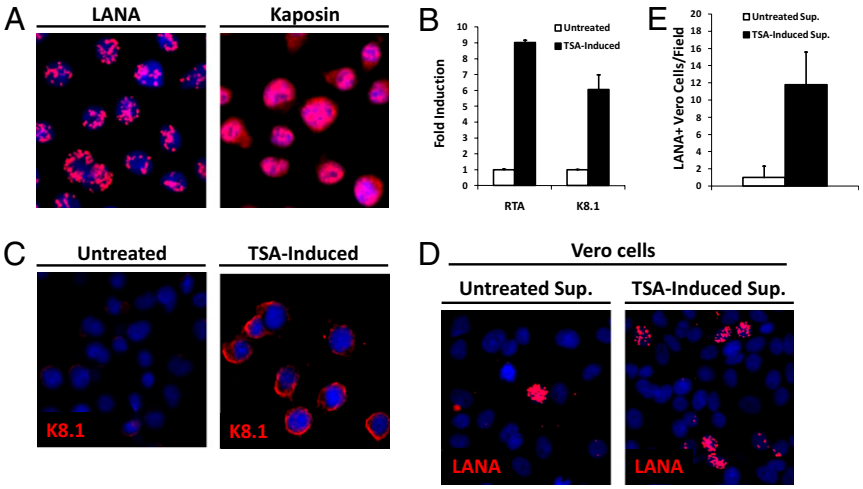

Fig. 2. UM-PEL-1 cells express KSHV antigens and produce infectious virions. (*A*) UM-PEL-1 cells stained for latent antigens LANA and Kaposin. (*B* and *C*) UM-PEL-1 cells were treated with Trichostatin A (TSA, 40 nM) for 72 h, and real-time qPCR was performed (*B*) as well as immunostaining of late lytic antigen K8.1 (*C*). (*D*) LANA staining of Vero cells (KSHV-negative cell line) after exposure to supernatants from untreated or TSA-treated (400 nM) UM-PEL-1 cells. (*E*) Quantification of LANA-positive Vero cells after supernatant treatment. Ten fields were counted for each condition, and data represent means ± SD. LANA-positive Vero cells are indicative of KSHV de novo infection. All results are representative of three independent experiments.

and *D*). Although both drug treatments led to an induction of KSHV lytic replication, they did so in a temporally distinct manner. Specifically, lytic reactivation was evident at 1 d after bortezomib treatment and 7 d after doxorubicin treatment.

Bortezomib Does Not Affect Constitutive Activation of NF-κB in UM-PEL-1 Cells. The potent anti-PEL activity of bortezomib prompted us to examine several potential mechanisms for this effect. Bortezomib has been shown to induce apoptosis by several mechanisms, one being the inhibition of the NF-κB prosurvival transcription factor (21–24). Previous reports have shown that PELs may exhibit constitutive activation of NF-κB that is necessary for their survival (17, 25). We therefore examined the status of NF-κB activation in UM-PEL-1 cells freshly obtained from mice ascites. NF-κB EMSA showed intranuclear p50 and p65 proteins indicative of constitutive activation of NF-κB. The activation of this transcription factor could be inhibited by in vitro treatment with the selective NF-κB inhibitor Bay-11 (Fig. 5*A*). Treatment with bortezomib (20 μM), however, was not effective in inhibiting constitutive NF-κB activity, as evidenced by the continued presence of intranuclear p50 and p65 proteins.

Bortezomib Treatment Does Not Induce a Terminal Unfolded Protein Response. PELs, which exhibit a plasma cell-like gene expression signature, have been shown to constitutively exhibit a partially activated unfolded protein response (UPR) (26). The source of the activated UPR is unknown, because these lymphomas, unlike

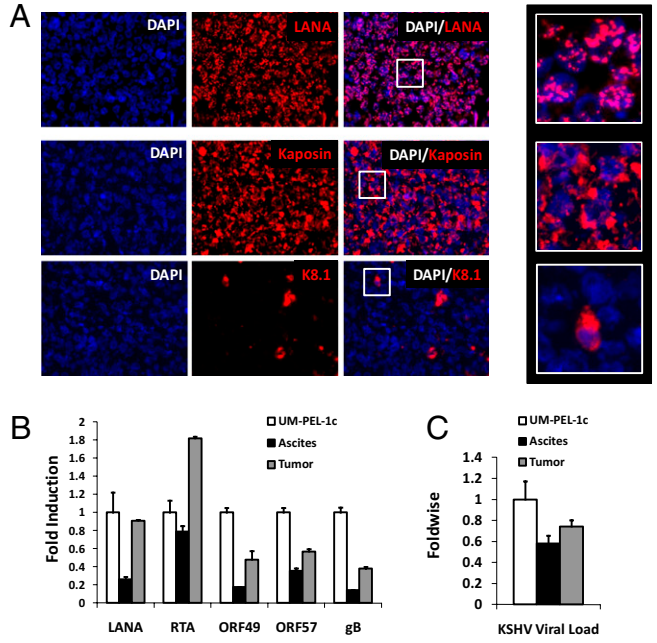

Fig. 3. KSHV gene expression is microenvironment dependent. (*A*) Frozen-section immunostaining of PEL solid lymphomas for LANA, Kaposin, and late lytic antigen K8.1. *Insets* show areas of stained tumors at higher magnification. (Magnification: *A*, ×400; *Insets*, ×1,600.) (*B* and *C*) In vitro-cultured UM-PEL-1c cells have higher viral loads than ascites and solid tumors. mRNA levels of KSHV latent and lytic genes were determined by qPCR analysis. Relative expression levels were normalized to in vitro-cultured UM-PEL-1c cells (*B*). DNA was isolated, and KSHV viral loads were determined by qPCR using LANA-specific primers (*C*). All results are representative of three independent experiments.

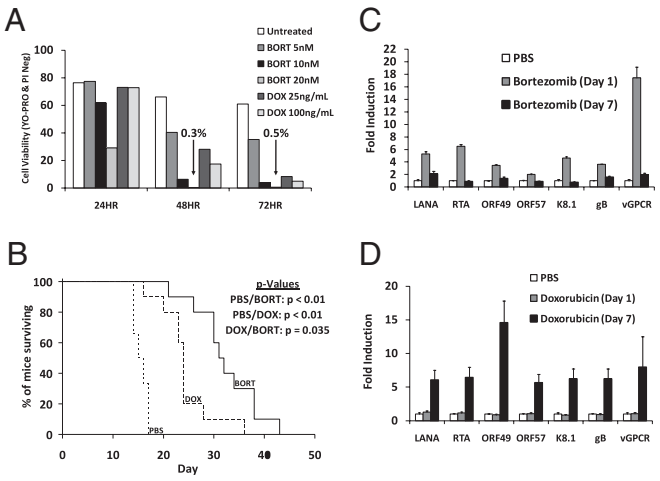

Fig. 4. Bortezomib potently induces apoptosis and lytic reactivation in UM-PEL-1 cells and improves overall survival of PEL mice. (*A*) In vitro-cultured UM-PEL-1c cells were treated with bortezomib or doxorubicin at the indicated doses. Cell viability was assayed by YO-PRO/PI staining and flow cytometric analysis at indicated time points. Results are representative of three independent experiments. (*B*) Mice were injected i.p. with 2×10^7 UM-PEL-1 cells. After 3 d mice were treated twice weekly for 3 wk with PBS, bortezomib (BORT) at 0.3 mg/kg, or doxorubicin (DOX) at 1.25 mg/kg. Mice were killed when moribund or showing signs of discomfort. Results are representative of two independent experiments. (*C* and *D*) UM-PEL-1 mRNA levels of latent, early, and late lytic genes were determined by qPCR and normalized to PBS control. Each group was composed of three mice. Bortezomib-treated (*C*) and doxorubicin-treated (*D*) mice were analyzed at day 1 and day 7 after treatment. Data from *C* and *D* represent means ± SD.

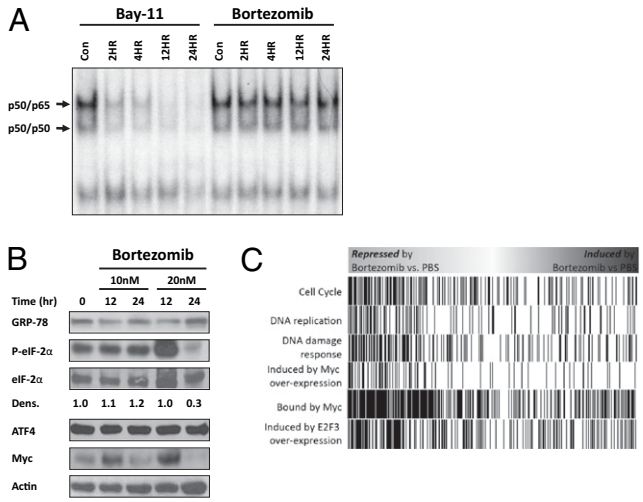

Fig. 5. Bortezomib does not inhibit NF-κB or induce a terminal UPR in UM-PEL-1 cells but does induce changes in transcriptional programs. (*A*) Immediately after removal from lymphoma-bearing mice, UM-PEL-1 cells were treated with the NF-κB inhibitor Bay-11 (5 μM) or proteasome inhibitor bortezomib (20 nM) for the indicated time periods. Nuclear extracts were prepared and assayed by EMSA using NF-κB–specific consensus oligonucleotides as probes. Results are representative of three independent experiments. (*B*) UM-PEL-1c cells were treated with bortezomib for the specified time periods. Whole-cell lysates were prepared, and Western blots were performed with specified antibodies. Immunoblotting for actin served as a loading control. Normalized densitometry of the phosphorylated eIF-2α (p-eIF-2α)/eIF-2α ratio is shown. The value in untreated cells was defined arbitrarily as 1. The results are representative of three independent experiments. (*C*) Sets of genes whose expression is significantly repressed by treatment with bortezomib compared with PBS. The top bar (not to scale) represents the ranked list of all genes ordered by their expression in bortezomib-treated versus PBS-treated PEL. Vertical black bars represent the ranking of member genes of the indicated gene sets. All FDRs < 0.001; see also Table S2.

plasma cells, do not express Ig protein (27). It has been shown that apoptosis and cell death can be induced in cells exhibiting an activated UPR by inhibiting the 26S proteasome (21). We therefore examined the expression of several UPR-associated proteins in UM-PEL-1 cells after treatment with bortezomib. GRP78 is an endoplasmic reticulum (ER) molecular chaperone that is up-regulated during a physiological, or nonterminal, UPR (28). We observed constitutive expression of GRP78 in UM-PEL-1 cells, indicative of an activated UPR, but no further induction of protein levels after bortezomib treatment (Fig. 5*B*).

Cells undergoing extensive ER stress frequently block de novo protein synthesis via phosphorylation of eukaryotic initiation factor 2α (eIF-2α) (29). Bortezomib treatment did not result in enhanced phosphorylation of eIF-2α (Fig. 5*B*), suggesting that inhibiting the 26S proteasome in PEL did not significantly enhance ER stress. We did observe an increase in total eIF-2α protein levels in cells treated with 20 nM bortezomib for 12 h; this transient effect may have been caused by inhibition of eIF-2α degradation by the 26S proteasome.

Activating transcription factor 4 (ATF4) frequently is associated with terminal UPR induction which up-regulates expression of proapoptotic GADD153/CHOP (30). ATF4 levels remained constant during bortezomib treatment (Fig. 5*B*), further suggesting that this drug does not induce apoptosis by activating a terminal UPR in UM-PEL-1 cells.

In Vivo Bortezomib Treatment Down-Regulates Expression of Genes Regulated by c-myc and E2F3 as well as Cell-Cycle Progression and DNA Replication Genes. To examine further the mechanism of the bortezomib-induced apoptosis, we carried out gene-expression profiling of UM-PEL-1 cells. The microarray analysis was conducted on mice bearing UM-PEL-1 xenografts after treatment for 24 h with PBS or bortezomib. We used Gene Set Enrichment Analysis (GSEA) to identify gene sets that were concordantly induced or repressed by treatment with bortezomib, compared with treatment with PBS (Fig. 5C and Table S2). Bortezomib significantly repressed genes involved in cell-cycle progression, DNA replication, and response to DNA damage stimuli. [All false discovery rates (FDRs) < 0.001.] Furthermore, genes induced by Myc or E2F3 forced expression, and genes that are bound by Myc in human B cells as determined by ChIP paired-end ditags (ChIP-PET) (31, 32) also were repressed by bortezomib. A total of 1,248 individual known genes were repressed at least 2-fold (mean, 3.5-fold; maximum, 41-fold) in bortezomib- versus PBS-treated cells, whereas 502 were up-regulated (mean, 2.8-fold; maximum, 34-fold). Many of these genes were modulated similarly by bortezomib treatment of Adult T-cell Leukemia (ATL) cells (Fig. S4) (33). The correlation between expression levels of these genes in our experiment compared with bortezomib-treated ATL cells was 0.61 ($P < 0.0001$). Analysis of the direction of changes in gene expression in the experiments also showed strong concordance ($P < 0.0001$ by χ^2-test).

As mentioned, targets of the Myc transcription factor were shown to be down-regulated after 24 h of bortezomib treatment in the gene-expression analysis. In agreement with the array results, we observed down-regulation of Myc protein levels after 24 h of bortezomib treatment (Fig. 5*B*). Interestingly, bortezomib treatment led to a transient induction in Myc levels at 12 h before subsequent down-regulation.

We also examined the effects of bortezomib on the phosphorylation status of Akt and JNK. No activation of JNK and Akt was observed in untreated or bortezomib-treated UM-PEL-1 cells (Fig. S5).

Discussion

Significant challenges, including disease rarity and lack of adequate models, have hindered progress in understanding PEL oncogenesis and evaluating new therapies. We set out to develop an in vivo model of this lymphoma that could reflect better the biology of the tumor without potential artifacts introduced by in vitro cell propagation. We directly transplanted PEL cells collected from the pleural effusion of a patient into the peritoneal cavities of immunodeficient NOD/SCID mice without ex vivo culture. This model may reflect the in vivo characteristics of this disease more accurately, as demonstrated by culture-induced changes in KSHV gene expression, and can be used to assess the efficacy of new therapeutic approaches. In addition, our study demonstrates the potent in vivo anti-PEL activity of bortezomib. Finally, we show that bortezomib as well as doxorubicin treatment can induce lytic reactivation of PEL in vivo. Our findings provide a strong basis for evaluation of bortezomib as a therapy for PEL in clinical trials.

The 26S proteasome inhibitor bortezomib is an effective treatment for several malignancies, including multiple myeloma (23) and mantle cell lymphoma (24). Bortezomib can induce apoptosis via several mechanisms, including NF-κB inhibition (17, 34), activation of a terminal UPR (21), and prevention of degradation of proapoptotic proteins and tumor-suppressor genes targeted for ubiquitination by KSHV during viral oncogenesis (22). Although bortezomib potently induced apoptosis of UM-PEL-1 cells, our in vitro results showed that it did not effectively block NF-κB activity. One possible explanation for the lack of NF-κB inhibition is the strong bortezomib-induced up-regulation of the KSHV early lytic gene *vGPCR*, which is a NF-κb activator (35).

It has been reported previously that PEL commonly exhibits a constitutively active UPR (26), and this UPR may potentially be exacerbated further by treatment with bortezomib to induce a terminal UPR and subsequent apoptosis (21). Although UM-PEL-1 cells exhibited constitutive ER stress, treatment with bortezomib did not induce a terminal UPR, thus suggesting that

the proapoptotic effects of this chemotherapy are mediated by another pathway in these cells.

Other survival pathways may be implicated in bortezomib-mediated apoptosis in UM-PEL-1 cells. KSHV genes *K1* and *vGPCR* can activate prosurvival Akt signaling to facilitate proliferation, survival, and tumorigenesis (36). Notably, some PEL cells have been shown to be dependent on this PI3K/Akt/mammalian target of rapamycin (mTOR) signaling axis for survival (37). Bortezomib-induced block of PI3K signaling leads to apoptosis, at least in hepatocellular carcinoma (38). However, we did not observe Akt activation in untreated or bortezomib-treated UM-PEL-1 cells.

We used gene-expression profiling to identify potential genes that are modulated by bortezomib treatment during induction of apoptosis. GSEA showed that several pathways are repressed by 24-h bortezomib treatment, including cell-cycle progression and DNA replication. In particular, the *RB1* and *PIM2* genes were repressed and may facilitate cell-cycle arrest in bortezomib-treated cells. In addition, we observed a strong repression of Myc target genes. Myc can be stabilized in PEL cells because of LANA-mediated inhibition of Myc phosphorylation and degradation (39). Myc stabilization has been shown to enhance proliferation, survival, and maintenance of the transformed state in the B-cell lineage (40, 41) and therefore may be essential for KSHV viral oncogenesis and lymphomagenesis. The down-regulation of Myc by bortezomib therefore may contribute to UM-PEL-1 cell death. It is important to note, however, that we observed a transient up-regulation of Myc protein levels by bortezomib at the 12-h time point. Myc also has a well-established role in induction of apoptosis (42, 43), and its up-regulation could have an effect on cell viability, as well. Further experiments to elucidate the role of Myc in bortezomib-treated UM-PEL-1 cells are necessary.

Our in vivo studies showed that bortezomib, as well as doxorubicin, was able to induce a lytic reactivation of KSHV within UM-PEL-1 cells that may result in viral replication and eventual tumor cell lysis. Indeed, others have shown that lytic reactivation of KSHV in PEL cells can be induced by various agents, such as TSA or butyrate, and may induce tumor cell lysis. Because of the difficulty of developing effective therapies for PEL, it has been proposed that inducing lytic reactivation of malignant cells during concomitant antiviral therapy may be an effective treatment approach (18). Our in vivo finding that bortezomib treatment can induce lytic reactivation of KSHV in PEL is in agreement with previous in vitro reports (44). Surprisingly, we also observed lytic reactivation after in vivo treatment with doxorubicin, although at a different time point. This finding stresses the need to study carefully the temporal dynamics of lytic activation induced by specific agents to optimize the potential benefit of adding antiviral drugs, such as ganciclovir or azidothymidine, to any front-line therapy. These antiviral nucleoside analogs have antiproliferative properties of their own when phosphorylated, a mechanism that can be exploited in the presence of HHV-8 thymidine kinase. The addition of antiviral drugs to bortezomib or doxorubicin therapy may increase clearance of PEL cells and improve survival.

Optimization of the therapeutic regimen for PEL has remained elusive because the rarity of the disease has prevented the launch of large-scale clinical trials. Additionally, patients diagnosed with PEL have an average survival of only 6 mo. It therefore is imperative that any clinical trials conducted for the evaluation of PEL therapies have a focused approach and include only therapies with the highest likelihood of success. Our UM-PEL-1 model will allow more in-depth studies of novel therapeutic approaches before their inclusion in clinical trials. Indeed, we used this model to compare directly the in vivo efficacy of bortezomib and doxorubicin, which commonly is used as a front-line therapy for PEL. Our results showed bortezomib to be significantly more effective in increasing overall survival of mice bearing PEL tumors. This finding correlated well with our in vitro data showing more robust activation of apoptosis by bortezomib than by doxorubicin, both delivered at clinically relevant concentrations. The in vivo efficacy of bortezomib, coupled with its favorable safety profile and lack of cardiotoxicity, provides a rational basis for testing this drug alone or in combination with antivirals in clinical trials of PEL.

Materials and Methods

Reagents. Bortezomib was obtained from Millennium Pharmaceuticals, and doxorubicin was purchased from Sigma-Aldrich. P-eIF2α, eIF2α, GRP78, pAkt, and Myc antibodies were purchased from Cell Signaling Technologies. ATF4, pJNK, and actin antibodies were purchased from Santa Cruz Biotechnology. CD3, CD19, CD20, CD30, CD38, CD45, CD79a, CD138, and HLA-DR antibodies were purchased from Beckman Coulter.

UM-PEL-1 Cells. Pleural effusion collected during the diagnostic tap of the patient with PEL was centrifuged over Ficoll/Paque gradient following the manufacturer's instructions (GE Healthcare) and was resuspended in effusion fluid. PEL cells (2×10^7) were injected i.p. into 6- to 8-wk-old female NOD/SCID mice (Jackson Laboratory). Mice were monitored daily for tumor growth. After 5–7 d, mice developed peritoneal swelling and were killed. A portion of the ascites was removed immediately postmortem via paracentesis; these cells are referred to as "UM-PEL-1" cells. For propagation, UM-PEL-1 cells were injected into the peritoneal cavities of additional NOD/SCID mice without ex vivo culture.

Cell Lines. For in vitro studies, UM-PEL-1 cells collected from mice were cultured in RPMI medium 1640 (Mediatech,) supplemented with 10% FBS (Mediatech), 2 nM glutamine (Gibco BRL), and penicillin/streptomycin (Gibco BRL). Cells cultured in vitro are referred to as "UM-PEL-1c" cells. The KSHV-positive, EBV-negative BC-3 PEL cell line derived from an HIV-negative patient (45) also was cultured in the supplemented RPMI medium 1640. 293T cells were cultured in DMEM supplemented with 10% FBS, 2 nM glutamine, and penicillin/streptomycin.

NF-κB EMSA and Apoptosis Studies. UM-PEL-1 cells were isolated from peritoneal cavities of mice harboring lymphomatous effusions by paracentesis, were placed into culture, and were treated with either Bay-11 or bortezomib. Cells (5×10^6) were collected at the indicated time points and used for nuclear protein extraction and EMSA supershift analyses as described previously (46) and summarized briefly in *SI Materials and Methods*.

For apoptosis studies, 10^5 cells/mL were incubated with or without bortezomib or doxorubicin for specified time periods, collected, washed with 1× PBS, and stained with propidium iodide (PI) (Invitrogen) and YO-PRO (Invitrogen) following the manufacturer's instructions. Flow cytometric analysis was performed on a Becton-Dickinson LSR analyzer (BD Biosciences).

In Vivo Tumor Studies. UM-PEL-1 cells (2×10^7) isolated from ascites of tumor-bearing mice were resuspended in 250 μL ascites fluid and injected i.p. into additional NOD/SCID mice. Mice were assigned randomly to a treatment group and on day 3 began receiving i.p. injections of PBS, bortezomib (0.3 mg/kg), or doxorubicin (1.25 mg/kg). Mice were monitored daily and were killed when moribund or exhibiting signs of discomfort in accordance with institutional guidelines. All procedures with animals were conducted in conformity with an approved institutional animal protocol.

RNA Isolation and Real-Time Quantitative PCR. RNA was isolated with the RNeasy Plus kit (QIAGEN) and DNase treatment on columns. We transcribed 500 ng of RNA into cDNA using the Reverse Transcription System (Promega) and Random Primers (Promega) according to the manufacturer's instructions. Real-time quantitative PCR (qPCR) was performed using an ABI Prism 7000 Sequence Detection System (Applied Biosystems) with Sybr Green PCR Master Mix (New England Biolabs). Sequences of primer sets are given in *SI Materials and Methods*. Melting curve analysis was performed to verify specificity of products as well as water and RT controls in every run. Data were analyzed using the $\triangle C_t$ method as in Mutlu et al. (47). Target gene expression was normalized to GAPDH by taking the difference between Ct values for target genes and GAPDH ($\triangle\triangle$ Ct value). These values then were calibrated to that of the control sample to give the Ct value. The fold target gene expression is given by the formula: $2^{-}\triangle\triangle C_t$.

Analysis of IgG V_H gene rearrangement was done as previously reported (48).

Vero Cell Infections. UM-PEL-1 cells were induced with TSA at 40 nM for 48 h and then at 400 nM for 24 h. Supernatants were centrifuged three times at 500 × *g* for 10 min at 4 °C. One milliliter of supernatant was added to 2×10^5

Vero cells and incubated for 24 h. The medium was removed, and cells were washed three times with Dulbecco's PBS (Gibco BRL) and incubated for 72 h. LANA staining was performed as described below.

Immunofluorescence Staining, Western Blot Analysis, and Microarray Hybridization. Immunostaining was performed as previously described by Mutlu et al. (47). Whole-cell extracts were prepared by lysing 5×10^6 cells, and Western blot analysis was performed as previously described (49).

Microarray hybridization was performed using the Affymetrix Human Gene 1.0ST arrays. A brief description of the procedure and analysis is provided in *SI Materials and Methods*.

Statistical Analysis. Mice survival curves were estimated using the Kaplan–Meier product-limit method and were compared using the log-rank test. P values <0.05 were considered statistically significant.

ACKNOWLEDGMENTS. I.S.L. is supported by National Institutes of Health Grants CA109335 and CA122105, University of Miami Developmental Center for AIDS Research Parent Grant 5P30A1073961, the Dwoskin Family, and the Bankhead-Coley and Fidelity Foundations. J.C.R. is supported by University of Miami Developmental Center for AIDS Research Parent Grant 5P30A1073961. A.J.G. is supported by National Cancer Institute Integrative Cancer Biology Program 1U54CA149145-01. E.A.M. is supported by National Institutes of Health Grants CA75918 and CA136387.

1. Chang Y, et al. (1994) Identification of herpesvirus-like DNA sequences in AIDS-associated Kaposi's sarcoma. *Science* 266:1865–1869.
2. Cesarman E, Chang Y, Moore PS, Said JW, Knowles DM (1995) Kaposi's sarcoma-associated herpesvirus-like DNA sequences in AIDS-related body-cavity-based lymphomas. *N Engl J Med* 332:1186–1191.
3. Cesarman E, Knowles DM (1999) The role of Kaposi's sarcoma-associated herpesvirus (KSHV/HHV-8) in lymphoproliferative diseases. *Semin Cancer Biol* 9:165–174.
4. Carbone A, et al. (2005) Kaposi's sarcoma-associated herpesvirus/human herpesvirus type 8-positive solid lymphomas: A tissue-based variant of primary effusion lymphoma. *J Mol Diagn* 7:17–27.
5. Simonelli C, et al. (2003) Clinical features and outcome of primary effusion lymphoma in HIV-infected patients: A single-institution study. *J Clin Oncol* 21:3948–3954.
6. Jones D, et al. (1998) Primary-effusion lymphoma and Kaposi's sarcoma in a cardiac-transplant recipient. *N Engl J Med* 339:444–449.
7. Chen YB, Rahemtullah A, Hochberg E (2007) Primary effusion lymphoma. *Oncologist* 12:569–576.
8. Judde J-G, et al. (2000) Monoclonality or oligoclonality of human herpesvirus 8 terminal repeat sequences in Kaposi's sarcoma and other diseases. *J Natl Cancer Inst* 92:729–736.
9. Ballestas ME, Kaye KM (2001) Kaposi's sarcoma-associated herpesvirus latency-associated nuclear antigen 1 mediates episome persistence through cis-acting terminal repeat (TR) sequence and specifically binds TR DNA. *J Virol* 75:3250–3258.
10. Renne R, et al. (1996) Lytic growth of Kaposi's sarcoma-associated herpesvirus (human herpesvirus 8) in culture. *Nat Med* 2:342–346.
11. Sun R, et al. (1999) Kinetics of Kaposi's sarcoma-associated herpesvirus gene expression. *J Virol* 73:2232–2242.
12. Guasparri I, Keller SA, Cesarman E (2004) KSHV vFLIP is essential for the survival of infected lymphoma cells. *J Exp Med* 199:993–1003.
13. Boulanger E, et al. (2005) Prognostic factors and outcome of human herpesvirus 8-associated primary effusion lymphoma in patients with AIDS. *J Clin Oncol* 23: 4372–4380.
14. Toomey NL, et al. (2001) Induction of a TRAIL-mediated suicide program by interferon alpha in primary effusion lymphoma. *Oncogene* 20:7029–7040.
15. Wu W, Rochford R, Toomey L, Harrington W, Jr, Feuer G (2005) Inhibition of HHV-8/KSHV infected primary effusion lymphomas in NOD/SCID mice by azidothymidine and interferon-alpha. *Leuk Res* 29:545–555.
16. Keller SA, Schattner EJ, Cesarman E (2000) Inhibition of NF-kappaB induces apoptosis of KSHV-infected primary effusion lymphoma cells. *Blood* 96:2537–2542.
17. An J, Sun Y, Fisher M, Rettig MB (2004) Antitumor effects of bortezomib (PS-341) on primary effusion lymphomas. *Leukemia* 18:1699–1704.
18. Klass CM, Krug LT, Pozharskaya VP, Offermann MK (2005) The targeting of primary effusion lymphoma cells for apoptosis by inducing lytic replication of human herpesvirus 8 while blocking virus production. *Blood* 105:4028–4034.
19. Staudt MR, et al. (2004) The tumor microenvironment controls primary effusion lymphoma growth in vivo. *Cancer Res* 64:4790–4799.
20. Parravicini C, et al. (2000) Differential viral protein expression in Kaposi's sarcoma-associated herpesvirus-infected diseases: Kaposi's sarcoma, primary effusion lymphoma, and multicentric Castleman's disease. *Am J Pathol* 156:743–749.
21. Obeng EA, et al. (2006) Proteasome inhibitors induce a terminal unfolded protein response in multiple myeloma cells. *Blood* 107:4907–4916.
22. Nikrad M, et al. (2005) The proteasome inhibitor bortezomib sensitizes cells to killing by death receptor ligand TRAIL via BH3-only proteins Bik and Bim. *Mol Cancer Ther* 4: 443–449.
23. Richardson PG, et al.; Assessment of Proteasome Inhibition for Extending Remissions (APEX) Investigators (2005) Bortezomib or high-dose dexamethasone for relapsed multiple myeloma. *N Engl J Med* 352:2487–2498.
24. O'Connor OA, et al. (2005) Phase II clinical experience with the novel proteasome inhibitor bortezomib in patients with indolent non-Hodgkin's lymphoma and mantle cell lymphoma. *J Clin Oncol* 23:676–684.
25. Guasparri I, Wu H, Cesarman E (2006) The KSHV oncoprotein vFLIP contains a TRAF-interacting motif and requires TRAF2 and TRAF3 for signalling. *EMBO Rep* 7:114–119.
26. Jenner RG, et al. (2003) Kaposi's sarcoma-associated herpesvirus-infected primary effusion lymphoma has a plasma cell gene expression profile. *Proc Natl Acad Sci USA* 100:10399–10404.
27. Drexler HG, Uphoff CC, Gaidano G, Carbone A (1998) Lymphoma cell lines: In vitro models for the study of HHV-8+ primary effusion lymphomas (body cavity-based lymphomas). *Leukemia* 12:1507–1517.
28. Lee AS (2005) The ER chaperone and signaling regulator GRP78/BiP as a monitor of endoplasmic reticulum stress. *Methods* 35 (4):373–381.
29. Rowlands AG, Panniers R, Henshaw EC (1988) The catalytic mechanism of guanine nucleotide exchange factor action and competitive inhibition by phosphorylated eukaryotic initiation factor 2. *J Biol Chem* 263:5526–5533.
30. Harding HP, et al. (2000) Regulated translation initiation controls stress-induced gene expression in mammalian cells. *Mol Cell* 6:1099–1108.
31. Zeller KI, et al. (2006) Global mapping of c-Myc binding sites and target gene networks in human B cells. *Proc Natl Acad Sci USA* 103:17834–17839.
32. Bild AH, et al. (2006) Oncogenic pathway signatures in human cancers as a guide to targeted therapies. *Nature* 439:353–357.
33. Hamamura RS, et al. (2007) Induction of heme oxygenase-1 by cobalt protoporphyrin enhances the antitumour effect of bortezomib in adult T-cell leukaemia cells. *Br J Cancer* 97:1099–1105.
34. Hideshima T, et al. (2001) The proteasome inhibitor PS-341 inhibits growth, induces apoptosis, and overcomes drug resistance in human multiple myeloma cells. *Cancer Res* 61:3071–3076.
35. Cannon ML, Cesarman E (2004) The KSHV G protein-coupled receptor signals via multiple pathways to induce transcription factor activation in primary effusion lymphoma cells. *Oncogene* 23:514–523.
36. Montaner S, Sodhi A, Pece S, Mesri EA, Gutkind JS (2001) The Kaposi's sarcoma-associated herpesvirus G protein-coupled receptor promotes endothelial cell survival through the activation of Akt/protein kinase B. *Cancer Res* 61:2641–2648.
37. Bhatt AP, et al. (2010) Dual inhibition of PI3K and mTOR inhibits autocrine and paracrine proliferative loops in PI3K/Akt/mTOR-addicted lymphomas. *Blood* 115: 4455–4463.
38. Chen KF, et al. (2009) Bortezomib overcomes tumor necrosis factor-related apoptosis-inducing ligand resistance in hepatocellular carcinoma cells in part through the inhibition of the phosphatidylinositol 3-kinase/Akt pathway. *J Biol Chem* 284: 11121–11133.
39. Bubman D, Guasparri I, Cesarman E (2007) Deregulation of c-Myc in primary effusion lymphoma by Kaposi's sarcoma herpesvirus latency-associated nuclear antigen. *Oncogene* 26:4979–4986.
40. Felsher DW, Bishop JM (1999) Reversible tumorigenesis by MYC in hematopoietic lineages. *Mol Cell* 4:199–207.
41. Wu M, et al. (1996) Inhibition of c-myc expression induces apoptosis of WEHI 231 murine B cells. *Mol Cell Biol* 16:5015–5025.
42. Nilsson JA, Cleveland JL (2003) Myc pathways provoking cell suicide and cancer. *Oncogene* 22:9007–9021.
43. Sarosiek KA, et al. (2010) Novel IL-21 signaling pathway up-regulates c-Myc and induces apoptosis of diffuse large B-cell lymphomas. *Blood* 115:570–580.
44. Brown HJ, McBride WH, Zack JA, Sun R (2005) Prostratin and bortezomib are novel inducers of latent Kaposi's sarcoma-associated herpesvirus. *Antivir Ther* 10:745–751.
45. Arvanitakis L, et al. (1996) Establishment and characterization of a primary effusion (body cavity-based) lymphoma cell line (BC-3) harboring Kaposi's sarcoma-associated herpesvirus (KSHV/HHV-8) in the absence of Epstein-Barr virus. *Blood* 88:2648–2654.
46. Kurokawa M, et al. (2005) Azidothymidine inhibits NF-kappaB and induces Epstein-Barr virus gene expression in Burkitt lymphoma. *Blood* 106:235–240.
47. Mutlu AD, et al. (2007) In vivo-restricted and reversible malignancy induced by human herpesvirus-8 KSHV: A cell and animal model of virally induced Kaposi's sarcoma. *Cancer Cell* 11:245–258.
48. Lossos IS, et al. (2000) Molecular analysis of immunoglobulin genes in diffuse large B-cell lymphomas. *Blood* 95:1797–1803.
49. Sarosiek KA, Nechushtan H, Lu X, Rosenblatt JD, Lossos IS (2009) Interleukin-4 distinctively modifies responses of germinal centre-like and activated B-cell-like diffuse large B-cell lymphomas to immuno-chemotherapy. *Br J Haematol* 147: 308–318.